Seismic Waves in the Asteroid Environment - Impactor Momentum Paul Sánchez[1]and Daniel J. Scheeres[2], [1]Colorado Center for Astrodynamics Research, University of Colorado Boulder, 3775 Discovery Dr, Boulder, CO 80303, [2]Ann and H.J. Smead Aerospace Engineering Sciences, University of Colorado Boulder, 3775 Discovery Dr, Boulder, CO 80303 (diego.sanchez-lana@colorado.edu).

By means of numerical simulations we investigate impact generated seismic wave transmission in granular media under extremely low pressure. This mimics the conditions in the interior of asteroids. We find that the wave induced pressure depends on the momentum of the impactor. This is an update and continuation to our abstract from 2020 [1].

Introduction: Experimentally, it is known that seismic waves speed in a granular medium is related to the overburden pressure (P) applied to it [2, 3]. The theory that has been developed is called Effective Medium Theory (EMT) and is based in considering the media as elastic, thus removing the difficulties presented by particle size and shape. This theory, based on the Hertzian laws for contacts, predicts a sound velocity that has a $P^{\frac{1}{6}}$ dependency, whereas the experiments have found this is true only for high enough pressures and that at low pressures the dependency changes to $P^{\frac{1}{4}}$. In fact, given that the sound speed for P and S waves are related to the elastic constants of the material, in the long wave limit, these can be written as:

$$v_p = \sqrt{\frac{K + 4/3\mu}{\rho}} \tag{1}$$

$$v_s = \sqrt{\frac{\mu}{\rho}} \tag{2}$$

where K is the bulk modulus, μ is the shear modulus and ρ is the density of the system. However, most experiments have been limited to kPa and MPa pressures as they have been carried out under Earth's gravity.

Small planetary bodies (asteroids, comets and small moons) produce gravitational fields in the *milli-* and *micro-g* regimes and, as a consequence, their interior pressure vary from zero (on their surface) to just a few Pascals or tens of Pascals in their innermost regions.

Soft-Sphere DEM: The simulation program that is used for this research applies a Soft-Sphere Discrete Element Method (SSDEM) [4], implemented as a computational code to simulate a granular aggregate [5, 6, 7, 8]. The particles, modelled as spheres that follow a predetermined size distribution, interact through a soft-repulsive potential when in contact. This method considers that two particles are in contact when they overlap. When this happens, normal and tangential contact forces are calculated [9]. The former is modelled by a hertzian spring-dashpot system and is always repulsive, keeping the particles apart; the latter is modelled with a linear spring that satisfies the local Coulomb yield criterion. The normal elastic force is modelled as

$$\vec{\mathbf{f}}_e = k_n \xi^{3/2} \hat{\mathbf{n}}, \tag{3}$$

the damping force as:

$$\vec{\mathbf{f}}_d = -\gamma_n \dot{\xi} \hat{\mathbf{n}}, \tag{4}$$

and the cohesive force between the particles is calculated as

$$\vec{\mathbf{f}}_c = -2\pi \frac{r_1^2 r_2^2}{r_1^2 + r_2^2} \sigma_{yy} \hat{\mathbf{n}} \tag{5}$$

where r_1 and r_2 are the radii of the two particles in contact, σ_{yy} is the tensile strength of this contact, which is given by a cohesive matrix formed by the (non simulated) interstitial regolith [10], and $\hat{\mathbf{r}}_{12}$ is the branch vector between the centres of these two particles. Then, the total normal force is calculated as $\vec{\mathbf{f}}_n = \vec{\mathbf{f}}_e + \vec{\mathbf{f}}_d$. In these equations, k_n is the elastic constant, ξ is the overlap of the particles, γ_n is the damping constant (related to the dashpot), $\dot{\xi}$ is the rate of deformation and $\hat{\mathbf{n}}$ is the vector joining the centres of the colliding particles. This dashpot models the energy dissipation that occurs during a real collision.

The tangential component of the contact force models surface friction statically and dynamically. This is calculated by placing a linear spring attached to both particles at the contact point at the beginning of the collision [9] and by producing a restoring frictional force $\vec{\mathbf{f}}_t$. The magnitude of the elongation of this tangential spring is truncated in order to satisfy the local Coulomb yield criterion $|\vec{\mathbf{f}}_t| \leq \mu |\vec{\mathbf{f}}_n|$.

Procedure: Here, we have chosen to use material parameters close to those of basalt so that the results are relevant for asteroids; the grains are spherical so

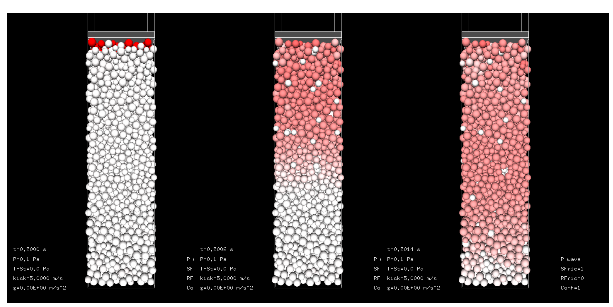

Figure 1: Simulation setup of a randomly packed aggregate; the redder the particle, the greater its vertical speed component (P=0.1 Pa).

that the results can also be related to sound transmission theory. We use 3120 grains with diameters between 2-3 cm that follow a uniform, random distribution for the randomly packed grains (RCP) (see Fig. 1) and 3570, 2.5 cm grains for the crystalline packing (HCP). Their density is 3200 kg m^{-3}, Young modulus is 7.8×10^{10} N m^{-2}, Poisson ratio is 0.25 [11]. Two coefficients of restitution are used: 0.1(settling) and 0.5 (wave transmission) to reduce the settling time.

The change in particle number was required so that the height of the columns remained the same for all simulations. The different particle arrangements implied different filling fractions and so, different bulk densities. However, we chose to keep the particle density the same and let the bulk density change as this more closely represents realistic laboratory conditions.

The particles are contained in a box with a solid bottom, horizontal periodic boundary conditions and a moving top that allows us to impose a very well determined pressure to the system. Though the particles initially settle under Earth's gravity, this is removed at a later stage to avoid pressure gradients. The height of the settled system is approximately 82 cm (see Fig. 1).

We will initiate the wave with the piston; we will change its thickness so changing its mass, we will also change its impact velocity. The thickness of the piston was set to: 2, 4 and 8 cm; the impact speed was: 0.1, 0.2, 0.4, 0.8 and 1.6 m/s. The nominal overburden pressure was kept at 1000 Pa to minimise the settling time and to keep the accuracy of the numerical method. The system is then divided into horizontal slices 5 cm thick to monitor energy transmission. The kinetic energy of each slice is calculated in order to observe the wave transmission. Data is collected every 5×10^{-5} s after the wave is started and this is done for 0.015 s. Sound speed is measured for the peak of the wave when it reaches the 2^{nd} slice from the bottom.

Results: Figs. 2 show semi-log plots of the pressure induced wave P_w vs. the momentum of the moving top (piston). We have also included three trend lines in each plot to make clear that the relationship between P_w and piston momentum is not linear. Notice that though we have 15 data points for each plot only 7 are evident in them as some of them are so close that they overlap. Meaning that, as long as the momentum of the impactor is the same, P_w will be the same. So then, for systems with the same overburden pressure, waves produced by impactors with the same momentum will be transmitted at the same speed. This is true for RCP and HCP systems. We also tried to do the same analysis relating P_w to the energy of the impactor, but this didn't render any evident relationship.

Unfortunately, from the fitting of our data, it is difficult to discern which non-linear fitting curve should be

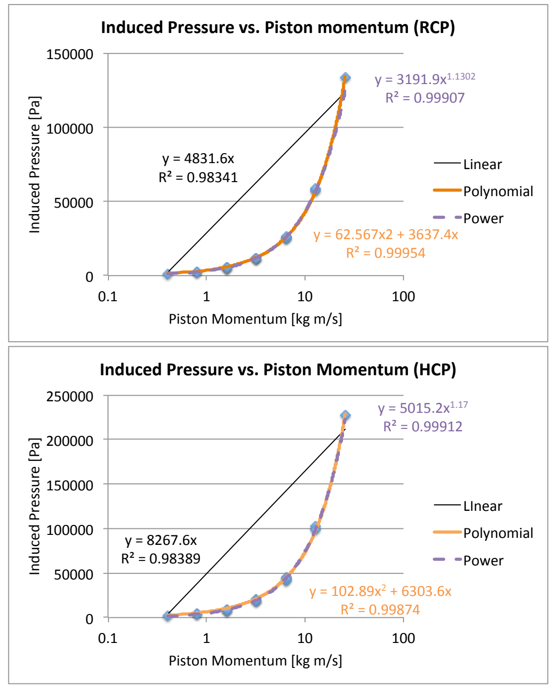

Figure 2: Wave-induced pressure vs. piston momentum for the RCP and HCP configurations. Three different trend lines have been included as well as their equations.

preferred. Both lines (polynomial and potential relationships) diverge for higher momenta and so the true dependency should come from a theoretical analysis of seismic waves transmission in granular media. This and other results will be presented at the conference.

References: [1] P. Sanchez, et al. (2020) in *Lunar and Planetary Science Conference* Lunar and Planetary Science Conference 1685. [2] K. Walton (1977) *Geophysical Journal International* 48(3):461 ISSN 0956-540X doi. [3] P. J. Digby (1981) *Journal of Applied Mechanics* 48(4):803. [4] P. Cundall (1971) in *Proceedings of the International Symposium on Rock Mechanics* vol. 1 129–136 -, Nancy. [5] P. Biswas, et al. (2003) *Phys Rev E* 68:050301(R). [6] P. Sánchez, et al. (2009) in *Lunar and Planetary Institute Science Conference Abstracts* vol. 40 of *Lunar and Planetary Inst. Technical Report* 2228–+. [7] P. Sánchez, et al. (2011) *The Astrophysical Journal* 727(2):120. [8] D. P. Sánchez, et al. (2012) *Icarus* 218(2):876 ISSN 0019-1035 doi. [9] H. Herrmann, et al. (1998) *Continuum Mechanics and Thermodynamics* 10:189 ISSN 0935-1175 10.1007/s001610050089. [10] P. Sánchez, et al. (2014) *Meteoritics & Planetary Science* 49(5):788 ISSN 1945-5100 doi. [11] B. Gundlach, et al. (2013) *Icarus* 223:479.